

Does the Brain's E:I Balance Really Shape Long-Range Temporal Correlations? Lessons Learned from 3T MRI

Lydia Sochan¹ and Alexander Mark Weber^{1,2,3*}

¹, School of Biomedical Engineering, The University of British Columbia,
Vancouver, BC, Canada.

², BC Children's Hospital Research Institute, The University of British
Columbia, Vancouver, BC, Canada.

³, Pediatrics, The University of British Columbia, Vancouver, BC, Canada.

*Corresponding author(s). E-mail(s): aweber@bcchr.ca;

Contributing authors: lydiasochan@gmail.com;

Keywords: Hurst exponent, long range temporal correlation, excitatory / inhibitory balance, criticality, complex systems, visual task, functional magnetic resonance imaging, magnetic resonance spectroscopy, functional magnetic resonance spectroscopy

¹ School of Biomedical Engineering, The University of British Columbia, Vancouver, BC, Canada

² BC Children's Hospital Research Institute, The University of British Columbia, Vancouver, BC, Canada

³ Pediatrics, The University of British Columbia, Vancouver, BC, Canada

* Correspondence: Alexander Mark Weber <aweber@bcchr.ca>

Abstract

A 3T multimodal MRI study of healthy adults ($n=19$; 10 female; 21.3 - 53.4 years) was performed to investigate the potential link between fMRI long-range temporal correlations and excitatory/inhibitory balance. The study objective was to determine if the Hurst exponent (H) — an estimate of the self-correlation and signal complexity — of the blood-oxygen-level-dependent signal is correlated with the excitatory-inhibitory (E:I) ratio. E:I has been proposed to serve as a control parameter for brain criticality, which H is believed to be a measure of. Thus, understanding if H and E:I are correlated would serve to clarify this relationship. Moreover, findings in this domain have implications for neurological and neuropsychiatric conditions with disrupted E:I balance, such as autism spectrum disorder, schizophrenia, and Alzheimer's disease. From a practical perspective, H is easier to accurately measure than E:I ratio at 3T MRI. If H can serve as a proxy for E:I, it may serve as a more useful clinical biomarker for this imbalance and for neuroscience research in general. The study collected functional MRI and magnetic resonance spectroscopy data during rest and movie-watching. H was found to increase with movie-watching compared to rest, while E:I did not change between conditions. H and E:I were not correlated during either movie-watching or rest. This study represents the first attempt to investigate this connection *in vivo* in humans. We conclude that, at 3T and with our particular methodologies, no association was found. We end with lessons learned and suggestions for future research.

1 Introduction

The brain is composed of individual neurons, each computationally-limited, that ultimately work together to produce astonishingly complex operations. Understanding how these neurons produce this emergent behaviour remains one of the great scientific challenges of our time. Recent advances in neuroscience have led to the emergence of the Critical Brain Hypothesis, which posits that the brain operates at a critical point, a state where order and disorder are balanced to enable the most efficient information processing [Deco et al., 2013, Beggs and Timme, 2012, Baranger, 2000, Bassett and Gazzaniga, 2011, Zimmern, 2020, Liang et al., 2024, Poil et al., 2012, Lombardi et al., 2017, Baumgarten and Bornholdt, 2019, Bruining et al., 2020, Trakoshis et al., Gao et al., 2017, Tian et al., 2022, Rubinov et al., 2011]. When in a critical state, the brain is optimally responsive to both internal and external stimuli while maintaining a balance between stability and instability [Deco et al., 2013, Beggs and Timme, 2012, Tian et al., 2022, Rubinov et al., 2011]. A fundamental theorem proposing how neural networks achieve this delicate balance centers around the excitation-inhibition (E:I) ratio: the balance of excitatory and inhibitory neural activity, often operationalized as the ratio of the primary excitatory and inhibitory neurotransmitters (i.e. glutamate (Glu) and γ -aminobutyric acid (GABA) [Liang et al., 2024, Lombardi et al., 2017, Baumgarten and Bornholdt, 2019, Bruining et al., 2020, Trakoshis et al., Gao et al., 2017]).

In vivo measurement of brain criticality can be achieved using several available methods, as systems near a critical state often exhibit fractal-like fluctuations or

scale-invariance [Muñoz, 2018]. Scale-invariance has been observed extensively across various neuronal spatio-temporal scales, from dendritic branching structures [Caserta et al., 1995] in the spatial domain, to neurotransmitter release [Lowen et al., 1997], neuronal firing rates [Mazzoni et al., 2007], local field potentials [Bédard and Destexhe, 2009], electroencephalography (EEG) [Bullmore et al., 1994] and functional magnetic resonance imaging (fMRI), which measures the blood oxygen level-dependent (BOLD) signal [Zarahn et al., 1997, Fadili and Bullmore, 2002, Campbell and Weber, 2022] in the time domain. This fractal structure can be quantified by assessing the signal's long-range temporal correlations (LRTC), which reflect the persistence or memory in a time series, where future values are statistically related to past values over long extended periods. The Hurst exponent (H) is a useful measure for evaluating LRTC [Eke et al., 2002, Campbell and Weber, 2022]. An H value between 0.5 and 1 indicates a long-range positive correlation, with large values being followed by large values and small values by small ones. Conversely, an H exponent value between 0 and 0.5 indicates a long-range negative correlation, where large values are likely to be followed by small ones and vice versa. An H value of 0.5 is uncorrelated random noise.

H has emerged as a valuable tool in neuroscience and clinical research. Typically, H values reported in adult brains are above 0.5, with higher H values in grey matter than white matter or cerebrospinal fluid [Dong et al., 2018, Wink et al., 2008]. Some key findings from neuroscience research include: a decrease in H during task performance [Ciuciu et al., 2014, He, 2011], negative correlations with task novelty and difficulty [Churchill et al., 2016], increases with age in the frontal and parietal lobes [Dong et al., 2018], and hippocampus [Wink et al., 2006], but decreases with age in the insula, and limbic, occipital and temporal lobes [Dong et al., 2018], and more [Campbell and Weber, 2022]. In terms of clinical findings, abnormal H values have been identified in Alzheimer's disease (AD) [Maxim et al., 2005, Warsi et al., 2012], autism spectrum disorder (ASD) [Dona et al., 2017a, Lai et al., 2010], mild traumatic brain injury [Dona et al., 2017b], major depressive disorder [Wei et al., 2013, Jing et al., 2017] and schizophrenia [Sokunbi et al., 2014]. Crucially, these same disorders have been associated with imbalances in E:I (AD: [Lauterborn et al., 2021, Vico Varela et al., 2019]; ASD [Sohal and Rubenstein, 2019, Uzunova et al., 2016, Bruining et al., 2020]; depression [Page and Coutellier, 2019]; and schizophrenia [Kang et al., 2019])

In addition to its implications for the critical brain hypothesis, establishing a connection between E:I and H could facilitate simpler estimation of excitatory and inhibitory neurotransmitters, as precise measurement of E:I is technically challenging [Ajram et al., 2019]. Currently, magnetic resonance spectroscopy (MRS) is the only non-invasive method for *in vivo* assessment of the Glu/GABA ratio (excitatory to inhibitory neurotransmitters) in humans [Stanley and Raz, 2018, Harris et al., 2017]. Unfortunately, MRS suffers from limited spatial and temporal resolution [Gao et al., 2017, Ajram et al., 2019, Stanley and Raz, 2018]. If H could function as a substitute for E:I, it would simplify the estimation of E:I in conditions of interest such as ASD, AD, and schizophrenia.

Going beyond clinical observations that imply a link between H and E:I, several studies have attempted to explore this association directly. However, they have primarily relied on computational models or animal studies [Liang et al., 2024, Poil et al., 2012, Lombardi et al., 2017, Baumgarten and Bornholdt, 2019, Bruining et al., 2020, Trakoshis et al., Gao et al., 2017]. To date, no *in vivo* study has validated this association in humans. Moreover, the existing research findings have so far been inconsistent, with some reporting positive-linear, negative-linear, or U-shaped relationships between the two variables. Therefore, further investigation is needed to establish the true nature of the potential E:I-Hurst relationship and to confirm its presence within the human brain. The current study aimed to explore the potential E:I-Hurst relationship *in vivo*, specifically within the visual cortex during movie-watching and resting periods.

2 Methods

2.1 Participants

Twenty-seven healthy adult participants were recruited to the study. One participant was not scanned due to feelings of claustrophobia while in the scanner. After our analysis and performing quality assurance (see below), a further seven participants were removed for having less than ideal MRI data quality, leaving nineteen final participants, between the ages of 21.3 and 53.4 (mean age \pm sd: 30.1 \pm 8.7 years; 9 males).

2.2 Ethics Statement

Written informed consent was obtained from all participants. Ethics approval was granted by the Clinical Research Ethics Board at the University of British Columbia and BC Children's & Women's Hospital (H21-02686).

2.3 Scanning Procedure

After two anatomical sequences were acquired, participants were instructed to visually fixate on a cross-hair for 24 minutes. During this period, an fMRI, single-voxel semi Localization by Adiabatic SElective Refocusing (sLASER) [Oz and Tkáč, 2011], and single-voxel MEscher-Garwood Point-REsolved SpectroScopy (MEGA-PRESS) [Mescher et al., 1998] sequences were acquired (see Figure 1 A and Section 2.4). Next, participants were instructed to watch a nature documentary (Our Planet (2019), Episode 3, “Jungles” Cordey [2019]) for 24 minutes. During this period, another set of fMRI, sLASER, and MEGA-PRESS sequences were acquired. See Figure 1 B for a visual representation of the scanning protocol. Total scan duration was approximately 1 hour. All participants followed the same order of rest than movie, and all participants saw the same movie segment, beginning at the same time during the scan.

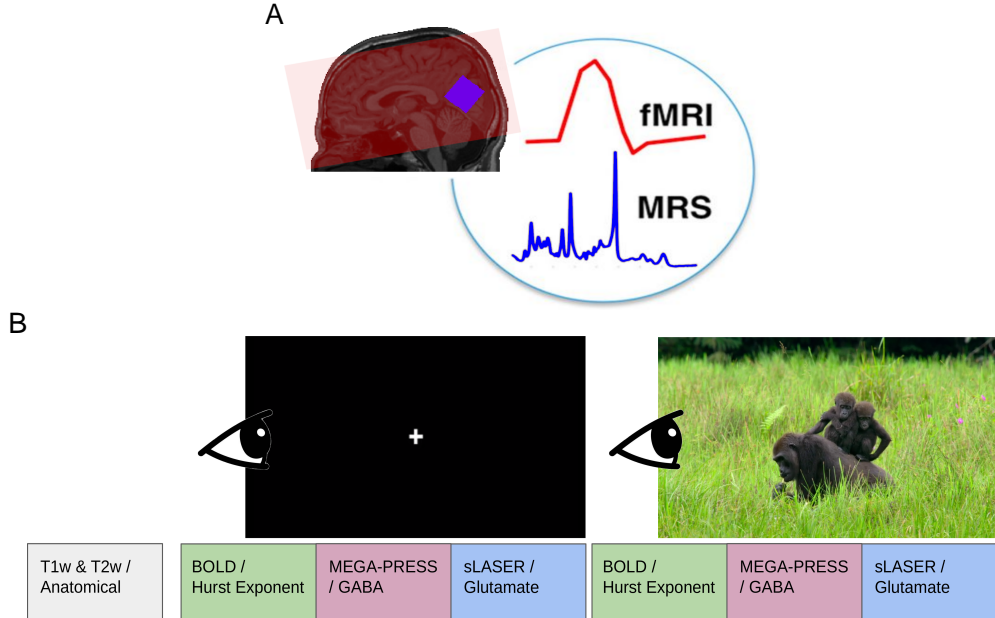


Figure 1. Overview of the MRI acquisition protocol. A) fMRI coverage was across the whole-brain (example coverage in red). MRS voxels were placed in the visual cortex (blue). Background image is of a T1w acquisition from a sample subject. B) fMRI, MEGA-PRESS and sLASER were acquired first with participants looking at a white cross for 24 mintues. Next, the same sequences were acquired with the participants viewing a nature documentary for an identical period of time.

2.4 Acquisition Details

Scans were performed at BC Children's Hospital MRI Research Facility on a 3.0 Tesla GE Discovery MR750 scanner (scanner software version: DV26.0_R03) with a Nova Medical 32 channel head coil. Participants changed into scrubs and were screened by an MRI technologist. Participants were given wax earplugs and a fiducial was placed on their left temple. Participants were provided with an audio headset and blanket once lying down on the scanner bed. Since visual stimuli were to be rear-projected, position and angle of mirror above patient eyes was adjusted for optimal movie viewing.

The following MRI scans were acquired. A 3D T1-weighted sagittal fast spoiled gradient echo (FSPGR) sequence; a 3D T2-weighted sagittal CUBE; a 2D echo-planar imaging (EPI) multi-echo gradient-echo fMRI sequence; a MEGA-PRESS sequence; and an sLASER sequence. Details are listed in Table 1.

Table 1. Summary of MRI acquisition details TE = echo time; TR = repetition time; FOV = field of view; FSPGD = fast spoiled gradient-echo; CUBE = a GE acronym; EPI = echo-planar imaging; fMRI = functional magnetic resonance imaging; sLASER = semi localization by adiabatic selective refocusing; MEGA-PRESS = Mescher-Garwood point-resolved spectroscopy

Sequence	TE (ms)	TR (ms)	Flip Angle	FOV	Slice Thickness (mm)	In-Plane Resolution (mm ²)	Other Parameters	Time (mins)
3D T1-weighted	2.176	7.216	12	256 × 256	0.9	0.9375 × 0.9375	-	5
FSPGR								
3D T2-weighted	75.242	2,504.090		256 x 256	0.9	0.9375 × 0.9375	-	4
CUBE								
2D EPI	12.2,	1,500	52	64 x 64	3.6	3.5938 × 3.5938	Acceleration factor = 6	12
Multi-Echo	35.352,							
fMRI	58.504							
MEGA-PRESS	68	1,800	90	-	28.0	28.0 x 28.0	-	4
sLASER	35	2,000	90	-	28.0	28.0 x 28.0	-	8

For both MRS sequences, the voxel size was set to 2.8 x 2.8 x 2.8 cm³. MRS voxels were rotated and placed in the occipital lobe, aligned along the calcarine fissure. Finally, blip-up and blip-down spin-echo versions of the fMRI sequence were acquired at the end to estimate the B0 non-uniformity map for fMRI phase distortion correction.

2.5 Image Processing

Our full image processing pipeline has been can be accessed from our Github account page: github.com/WeberLab/EI_Hurst_Analysis

Images were downloaded offline from the scanner in raw Digital Imaging and Communications in Medicine (DICOM) format. DICOM files were then converted to Neuroimaging Informatics Technology Initiative (NIfTI) using Chris Rorden's `dcm2niix` [Li et al., 2016] (v1.0.20211006) and then to Brain Imaging Data Structure (BIDS) [Gorgolewski et al., 2016a] format using `dcm2bids` [Boré et al., 2023] (v2.1.6).

2.5.1 Structural Images

The T1w image was corrected for intensity non-uniformity with `N4BiasFieldCorrection` [Tustison et al., 2010] and distributed using ANTs [Avants et al., 2008] (v2.3.335) to be used as a T1w-reference for the rest of the workflow. The T1w-reference was skull-stripped using a Nipype [Gorgolewski et al., 2016b]

implementation of `antsBrainExtraction.sh` from ANTs; OASIS30ANTS was used as a target template. `Fast` [Zhang et al., 2001] (FSL [Smith et al., 2004] v.6.0.5.1:57b01774, RRID: SCR_002823) was used for brain tissue segmentation into cerebrospinal fluid (CSF), white matter (WM), and gray matter (GM). Brain surfaces were reconstructed with `recon-all` [Dale et al., 1999] (`FreeSurfer` [Dale et al., 1999] 7.3.2, RRID: SCR_001847). The previously-estimated brain mask was refined with `Mindboggle` [Klein et al., 2017] (RRID:SCR_002438) to reconcile ANTs-derived and FreeSurfer-derived segmentations of cortical GM. `AntsRegistration` [Avants et al., 2008] (ANTs 2.3.3) was used to perform volume-based spatial normalization to two standard spaces: MNI152NLin2009cAsym and MNI152NLin6Asym. Normalization used brain-extracted versions of both T1w reference and T1w template.

2.5.2 fMRI

Using `fMRIPrep` [Esteban et al., 2019], the shortest echo of the BOLD run was used to generate a reference volume (both skull-stripped and skull-included). Head-motion parameters with respect to the BOLD reference (transformation matrices as well as six corresponding rotation and translation parameters) were estimated before spatiotemporal filtering using `mcflirt` [Jenkinson et al., 2002] (FSL v6.0.5.1:57b01774). The fieldmap was aligned with rigid registration to the target EPI reference run. Field coefficients were mapped to the reference EPI using the transform. BOLD runs were slice-time corrected to 643 ms (half of slice acquisition range of 0-1290 ms) using `3dTshift` from AFNI [Cox, 1996] (RRIS: SCR_005927). To estimate $T2^*$ map from preprocessed EPI echoes, a voxel-wise fitting was performed by fitting the maximum number of echoes with reliable echoes in a particular voxel to a monoexponential signal decay model with nonlinear regression. Initial values were $T2/S0$ estimates from a log-linear regression fit. This calculated $T2$ map was then used to optimally combine preprocessed BOLD across echoes using the method by Posse et al. (1999) [Posse et al., 1999]. The generated BOLD reference was then co-registered (6 degrees of freedom) to the T1w reference with `bbregister` (`FreeSurfer` [Dale et al., 1999]) using boundary-based registration. First, a reference volume and its skull-stripped equivalent were generated with `fMRIPrep`. Confounding time series were calculated from preprocessed BOLD: framewise displacement (FD), DVARS, and three region-wise global signals. `Tedana` [DuPre et al., 2021] was then used to denoise the data by decomposing the multi-echo BOLD data via principal component analysis (PCA) and independent component analysis (ICA). The resulting components are automatically analyzed to determine whether they are TE-dependent or -independent. TE-dependent components were classified as BOLD, while TE-independent components were classified as non-BOLD and were discarded as part of data cleaning.

Participants were excluded from further analysis if their mean FD was > 0.15 mm.

2.6 MRS

sLASER data were processed and fit to a spectrum using `Osprey` [Oeltzschner et al., 2020] (v2.4.0). Full width half-maximum (FWHM) of the single-Lorentzian fit of the N-acetylaspartate (NAA) peak were calculated for quality assurance purposes. The MRS

voxel was co-registered to T1w reference image and segmented by SPM12 [Friston et al., 2007] into CSF, GM, and WM. Metabolites were water-scaled as well as tissue- and relaxation-corrected by the Gasparovic et al. (2006) method [Gasparovic et al., 2006]. Glutamate is challenging to capture due to its signal overlaps with other metabolites [Pasanta et al., 2023]. In particular, Glu shares a similar chemical structure with glutamine (Gln) which causes the spectral features of Glu to be contaminated with Gln [Ramadan et al., 2013]. As a result, we decided to report Glx values, which co-reports Glu and Gln to avoid errors in spectral assignment, especially since it is controversial whether Glu can reliably be separated from Gln at 3T [Pasanta et al., 2023, Ramadan et al., 2013]. We henceforth refer to Glu as either Glx.

MEGA-PRESS data were processed and fit with Osprey, and were relaxation-, tissue- and alpha-corrected using the Harris et al. (2015) method [Harris et al., 2015]. Osprey values were ultimately used for further analysis. Due to the J-editing sequence of MEGA-PRESS, a challenge of GABA quantification is macromolecule quantification [Harris et al., 2015]. As a result, we report GABA+, a measure which co-reports GABA with macromolecules. Macromolecules (MM) are expected to account for approximately 45% of the GABA+ signal [Harris et al., 2015]. While a macromolecule-suppressed estimate of GABA seems ideal, a recent 25-site and multi-vendor study conducted at 3T found that GABA+ showed much lower coefficient of variation than MM-suppressed GABA, meaning that GABA+ is more consistent across research sites and MRI vendors (i.e., Philips, GE, Siemens) [Mikkelsen et al., 2019]. Moreover, GABA+ shows greater reliability for both creatine-referenced and water-suppressed estimates [Mikkelsen et al., 2017, 2019]. MM-suppressed GABA and GABA+ estimates are also correlated, albeit weakly- to moderately-so [Harris et al., 2015, Mikkelsen et al., 2019, 2017]. Consequently, we report GABA+ to allow for easier comparison of our results to other studies as well as reproducibility.

Basis sets were created using MRSCloud [Hui et al., 2022, Mori et al., 2016]. For sLASER, ‘localization’ was set to ‘sLASER’, ‘vendor’ to ‘GE’, ‘editing’ to ‘UnEdited’, and ‘TE’ to 35. For MEGA-PRESS, ‘localization’ was set to ‘PRESS’, ‘editing’ to ‘MEGA’, ‘TE’ to 68, ‘edit on’ to ‘1.9’, ‘edit off’ to ‘7.5’, and ‘pulse duration’ to ‘14’. Metabolites included for both basis sets were: Asc, Asp, Cr, CrCH₂, EA, GABA, GPC, GSH, Gln, Glu, Gly, H₂O, Lac, NAA, NAAG, PCh, PCr, PE, Ser, Tau, mI, and sI. Excitatory-inhibitory ratio (E:I) was calculated as [Glx in i.u.]/[GABA+ in i.u.], a common practice to report E:I using MRS [Rideaux, 2021].

Participants were excluded from further analysis if any of their MRS scans had FWHM > 10. Originally we intended to calculate, report and analyze MRS as tissue-corrected quantitative values. However, the Osprey software was reporting Glx values that were an order of magnitude larger than reported values in the literature. Despite several attempts, we were unable to locate the source of this error. Therefore we decided to use metabolite to creatine ratios (i.e. Glx / tCr and GABA+ / tCr) to be safe.

2.7 Hurst Exponent Calculation

Hurst exponent was calculated from the power spectrum density (PSD) of the BOLD signal. A log-log plot was used, where log power was plotted against log frequency; generally, if a log-log plot results in a linear relationship, it is assumed that the mean slope of this line represents the power-law exponent [Zimmern, 2020]. A PSD shows the distribution of signal variance ('power') across frequencies. Complex signals are classified into two categories: fractional Gaussian noise (fGn) and fractional Brownian motion (fBm) [Duff et al., 2008, Eke et al., 2002]. The former is a stationary signal (i.e., does not vary over time), while the latter is non-stationary with stationary increments [Eke et al., 2002]. Most physiological signals consist of fBm, but fMRI BOLD is typically conceptualized as fGn once motion-corrected; otherwise put, unprocessed BOLD signal is initially fBm which is converted to fGn with appropriate processing [Bullmore et al., 2004]. fBm and fGn require distinct H calculation methods [Eke et al., 2002]. PSD was estimated using Welch's method [Welch, 1967] from the Python Scipy.Signal library [Virtanen et al., 2020]. Data were divided into 8 windows of 50% overlap and averaged. The spectral index, β , was calculated from the full frequency spectrum. The spectral index was then converted to H using the following equation [Eke et al., 2002, Schaefer et al., 2014]:

$$H = \frac{1 + \beta}{2}$$

Since it cannot be assumed that all fBm is removed from the signal, we use the concept of 'extended Hurst' (H') in this study: for $0 < H < 1$, the signal is understood as fGn, while for $1 < H < 2$, the signal is assumed to be fBm [Campbell et al., 2022]. More generally, it is also assumed that when $0.5 < H < 1.5$, the signal displays 1/f behaviour [Zimmern, 2020]. H was calculated for all voxels in the brain of each subject. A brain mask was then applied which included only GM and the region of the MRS voxel in the visual cortex. H was averaged across the brain mask area, using only non-zero voxels.

2.8 Statistics

All statistical analyses were performed using R [Team, 2021] and RStudio (v2023.06.0+421). Difference of means between rest and movie conditions were calculated using paired Student's t-tests [Student, 1908]. Correlations were calculated using Pearson's method [Freedman et al., 2007]. Finally, linear mixed-effect models were used to test for more complicated models.

3 Results

3.1 Participant Demographics

Twenty-seven participants were originally recruited for the study. Twenty-six of these participants were successfully scanned, but one participant experienced anxiety and chose not to continue. Of the remaining 26 participants, 19 were included in the final

analysis: two were removed due to low MRS quality ($\text{FWHM} > 10$) and five were removed due to low fMRI quality (mean FD > 0.15 mm). See Figure 2.

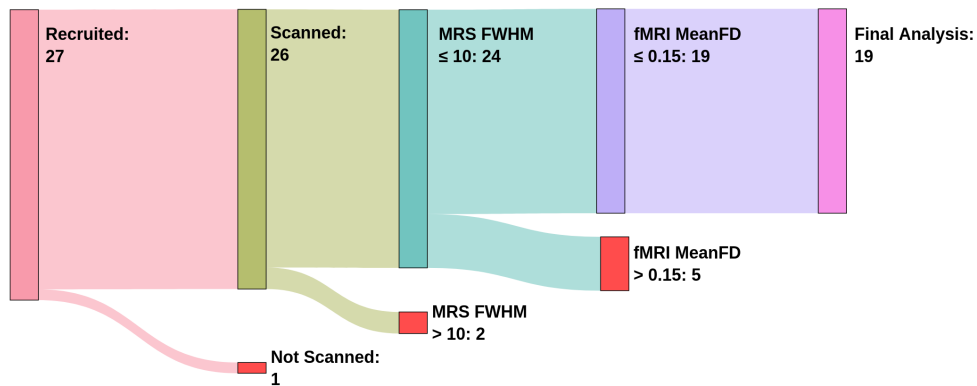


Figure 2. Flowchart of participant, recruitment, scanning and exclusion. The number of participants at each stage is indicated within each node. Participants were excluded based on MRS FWHM and fMRI Mean FD thresholds, resulting in 19 participants included in the final analysis

The final study sample included 9 males and 10 females between ages 21.3 and 53.4, with a mean age and standard deviation of 30.1 ± 8.7 years.

3.2 Data Quality

After exclusion, FWHM (mean \pm sd) at rest in sLASER and MEGAPRESS were 8.52 ± 0.7 and 7.02 ± 0.7 , respectively. During movie watching, FWHM in sLASER and MEGAPRESS were 8.37 ± 0.65 and 6.98 ± 0.86 .

Glx and GABA+ were tested for associations with FWHM values during rest and movie watching. Glx during rest was found to be negatively correlated with FWHM ($r = -0.53$, $p = 0.02$). No other correlations were significant.

An average of all MRS voxel placements can be seen in Figure 3 A, and a sample of the Osprey sLASER and MEGAPRESS spectrum fits at rest can be seen in Figure 3 B and C, respectively.

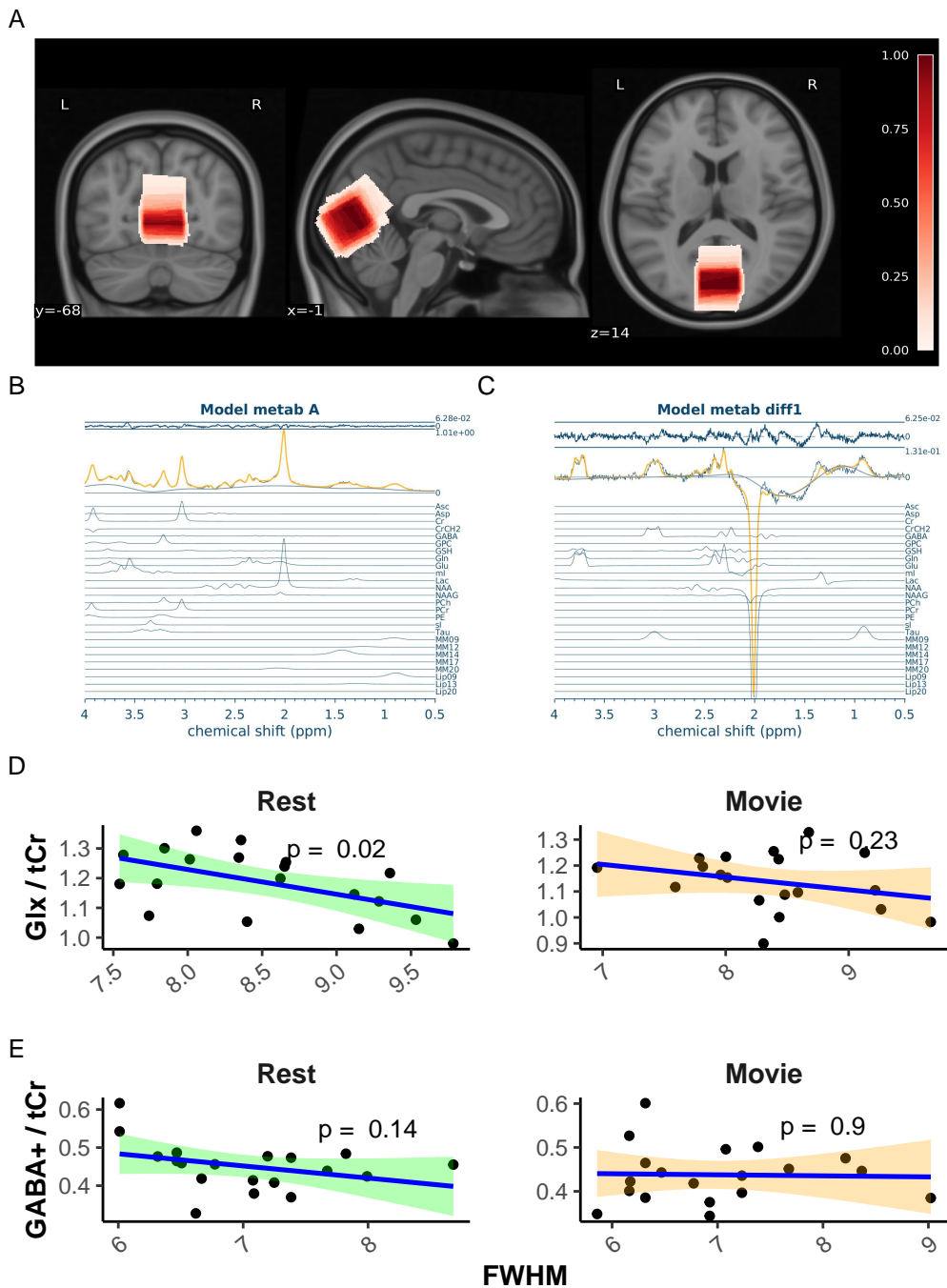


Figure 3. MRS data quality A) Average MRS location. Overlay in red of the average voxel location across all nineteen participants, from 0 (white) to 1 (dark red). Darker red represents voxel locations shared by all participants, while white represents voxel locations unique to participants. MRS voxels were registered to MNI space and averaged. Underlay is T1w MNI152 at 0.5 mm resolution. B) Sample Osprey sLASER Spectrum. Yellow spectrum indicates overall model fit. Model fits for individual metabolites are shown in blue below overall fit. C) Sample Osprey MEGAPRESS Spectrum. Yellow spectrum indicates overall model fit. Model fits for individual metabolites are shown in blue below overall fit. D) Correlation plots of Glx / tCr vs. FWHM for rest (green) and movie (red). E) Correlation plots of GABA+ / tCr vs. FWHM for rest (green) and movie (red).

A sample of the combined grey-matter and MRS voxel mask used to average H values, along with a sample Hurst exponent map, and sample fits for H calculation during rest can be found in Figure 4 A, B, and C, respectively.

Mean FD was not correlated with H during rest ($r = -0.33$, $p = 0.16$) but was moderately negatively correlated with H during movie watching ($r = -0.50$, $p = 0.03$; see Figure 4 D).

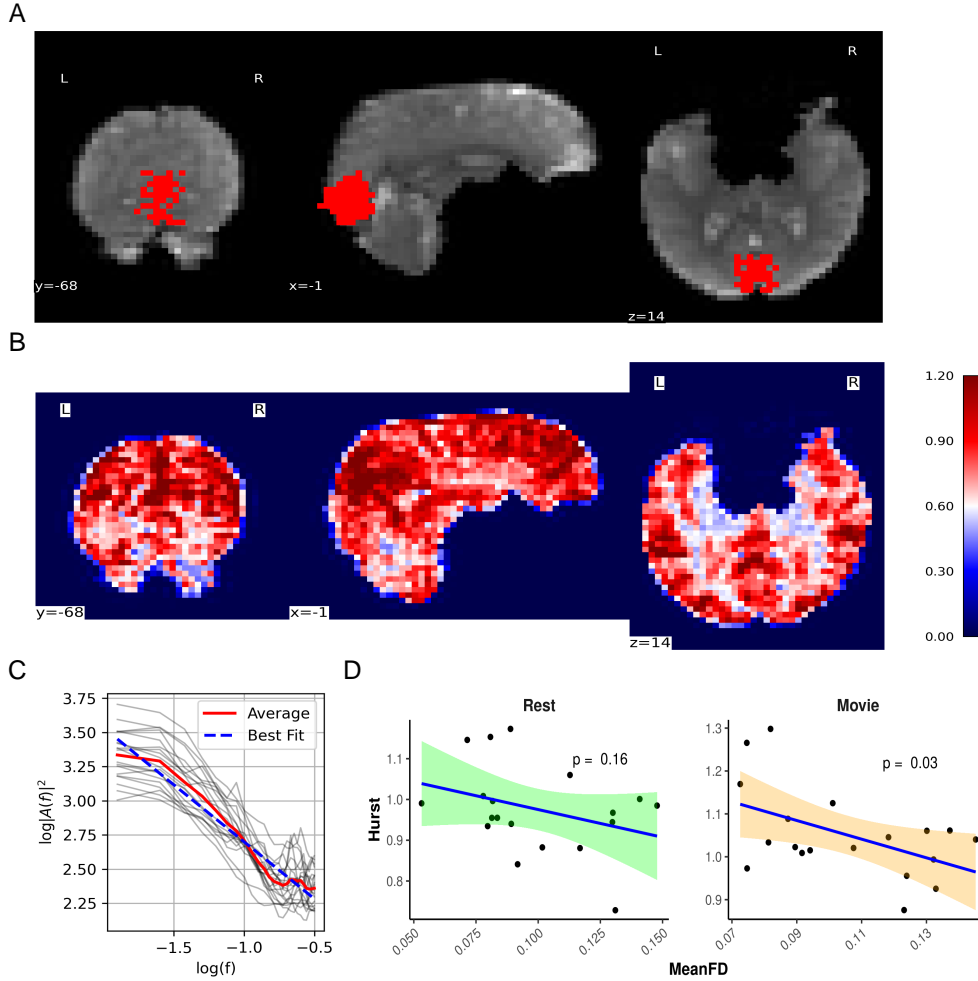


Figure 4. fMRI data quality. A) sample fMRI grey-matter mask within the MRS voxel. Background: a sample coronal, sagittal, and axial slice is displayed of the mean fMRI scan from the rest acquisition. Foreground: the greymatter/MRS mask used to calculate mean H. B) Sample H map for whole brain. Coronal, sagittal, and axial views are shown, colour-coded by H values. Colour-coding shows evident tissue differentiation by H value (i.e., gray matter (red), white matter (light red), and cerebrospinal fluid (white)). C) Sample PSD spectrum. All participants' PSD spectra during rest are plotted using light grey lines. Mean PSD is plotted in solid red Mean linear regression line is plotted in dashed blue. H for each participant was calculated from the slope of their mean linear regression line. D) Correlation plots of H vs. meanFD for rest (green) and movie (orange).

3.3 Relationship between H and E:I

Mean \pm sd of metabolites, E:I, and H during rest and movie are reported in Table 2. Boxplots between rest and movie can be seen in Figure 5. Neither Glx nor GABA+ were different between movie and rest conditions. E:I ratio did not change between conditions either. H was found to be greater during movie watching than rest.

Table 2. Summary of main results

	Rest	Movie	p-value
Glx / tCr	1.19 ± 0.11	1.14 ± 0.11	0.09
GABA+ / tCr	0.45 ± 0.06	0.44 ± 0.06	0.50
E:I Ratio	2.68 ± 0.49	2.65 ± 0.45	0.82
H	0.98 ± 0.98	1.05 ± 1.05	< 0.01

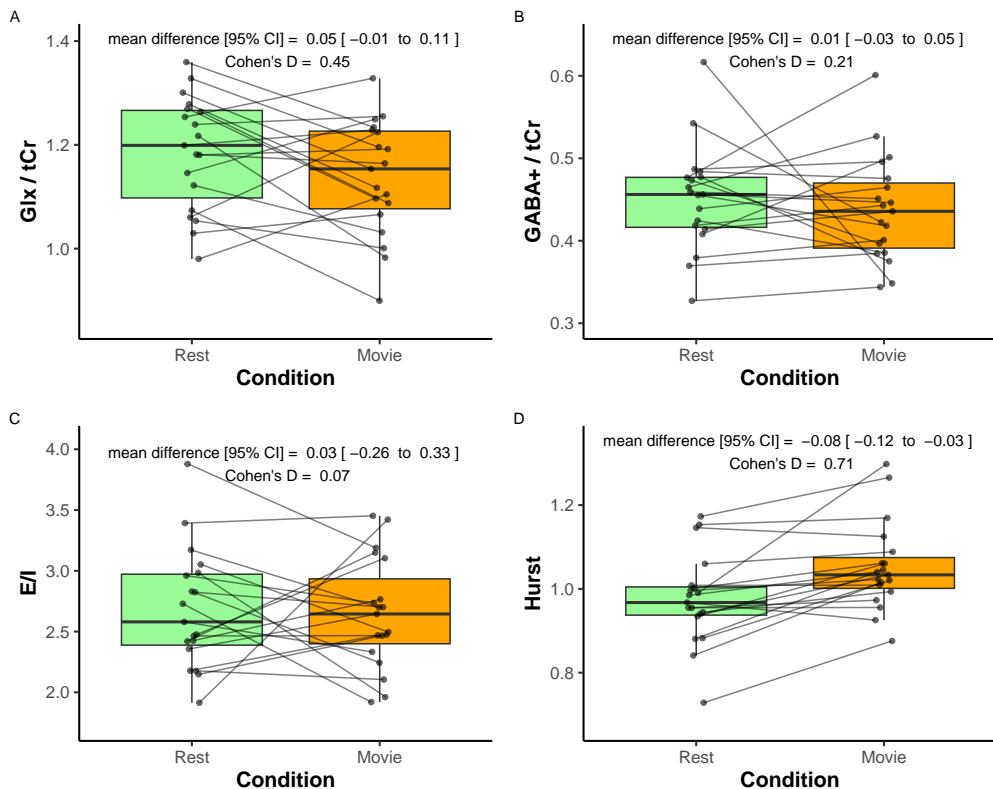


Figure 5. Paired comparison of metabolite values during rest (green) and movie (orange) conditions. A) Glx / tCr; B) GABA+ / tCr; and C) E:I. Paired dots represent the same participant across conditions. Mean difference with 95% confidence intervals, and as Cohen's D are reported at the top of each plot.

H was not found to correlate with Glx, GABA+, or E:I, during rest or movie (Figure 6).

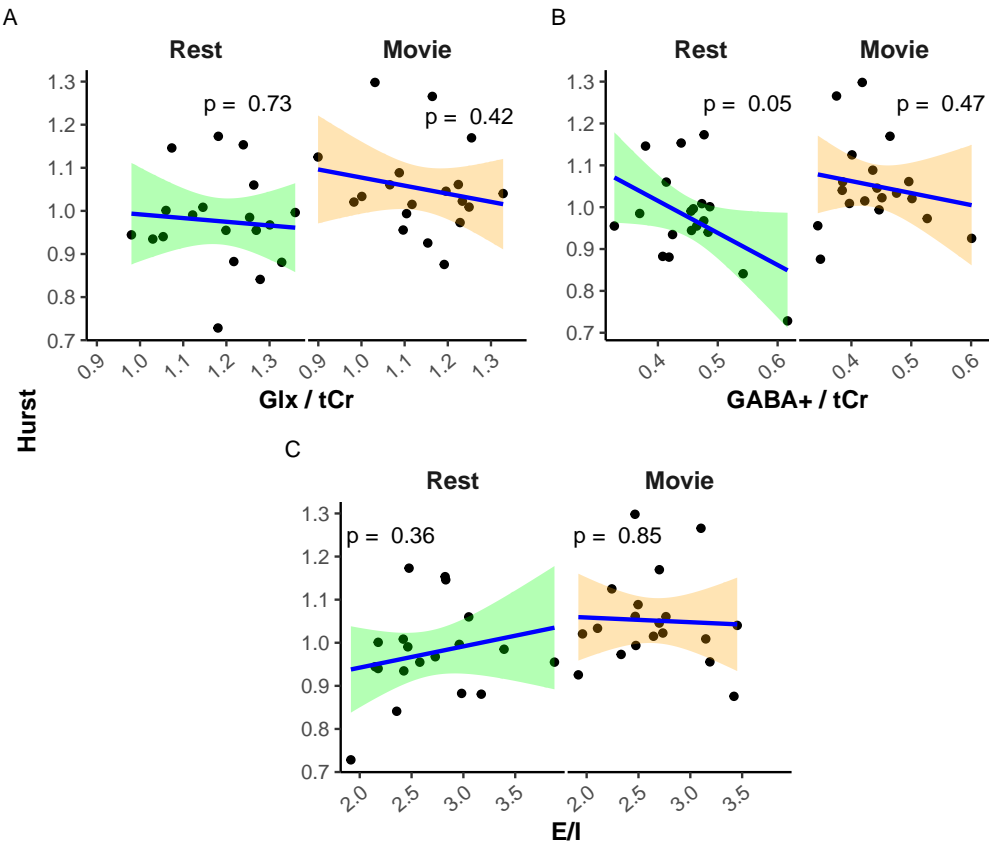


Figure 6. Scatter plots of H vs. metabolites. A) Glx / tCr; B) GABA+ / tCr; and C) E:I. Rest is in green, while movie is in orange. p-values are reported at the top of each plot.

To ensure that meanFD and FWHM were not confounding our results, we also ran a linear mixed-effects model with H as dependent variable, Glx/GABA+ as primary predictor of interest, and meanFD, FWHM(Glx), and FWHM(GABA+) as covariates, Condition (rest vs. movie) as fixed effects, and subjects as random effects:

$$H \sim \frac{\text{Glx}}{\text{GABA}+} + \text{meanFD} + \text{FWHM}_{\text{Glx}} + \text{FWHM}_{\text{GABA}+} + \text{Condition} + (1|\text{Subject})$$

The model's total explanatory power was substantial (conditional $r^2 = 0.69$), with fixed effects alone (marginal r^2) equal to 0.19. The model's intercept, corresponding to EI = 0, Condition = Movie, FWHMs_Glx_ = 0, FWHM_GABA+_ = 0 and meanFD = 0, was 0.98 (95% CI [0.41, 1.56], $t(30) = 3.34$, $p = 0.002$). Within this model, only the effect of Condition [Rest] was statistically significant ($\beta = -0.09$, 95% CI [-0.13, -0.04], $t(30) = -3.99$, $p < 0.01$).

4 Discussion

We report here the first *in vivo* human study of the E:I-H relationship. An increase in H was observed during movie-watching as compared to rest, indicating stronger long-range temporal dependencies in BOLD activity during visual stimulation. No difference was found in Glx, GABA+, nor Glx/GABA+ between rest and movie-watching. Furthermore, no association was found between H and Glx, GABA+, nor Glx/GABA+. Attempting to control for meanFD and FWHM using a linear mixed-effects model did not alter these results.

Our finding that H increases during movie-watching compared to rest is consistent with a previous study from our lab [Campbell et al., 2022], which reported increased H in the visual network (from Yeo's seven resting-state networks [Thomas Yeo et al., 2011]) during movie-watching using data from the Human Connectome Project [Van Essen et al., 2012]. While this increase in H is consistent with our prior findings, other studies have reported decreases in H during active tasks [He, 2011, Churchill et al., 2016, Ciuciu et al., 2014, Barnes et al., 2009]. Our results suggest that the naturalistic, passive nature of movie-watching elicits a different effect on H compared to more active tasks. This is consistent with literature indicating distinct neural responses and BOLD signal characteristics between conventional active visual tasks and naturalistic passive visual stimuli [Campbell et al., 2022, Hasson et al., 2010]. Richer scaling properties (higher H) during movie-watching may support the continuous perception of visual stimuli [Campbell et al., 2022].

We found no changes in either Glx or GABA+ between conditions. Given that no difference was observed for either metabolite, it is unsurprising that E:I did not change either. This was unfortunate as our study was designed to include two conditions in order to elicit changes in H, Glx, and GABA+, aiming to confirm that our experiment induced measurable alterations in these metrics. Establishing such changes would have provided a foundation for directly examining the correlation between H and the E/I ratio. However, because Glx and GABA+ did not show significant changes between conditions, our main results are likely to be met with doubt. Without evidence of condition-induced variations in Glx and GABA+, it remains unclear whether the absence of correlation reflects a true lack of association or insufficient sensitivity of our measurement approach to detect changes in these metabolites.

A recent meta-analysis of Glu/Glx studies [Pasanta et al., 2023] reported a minimal task-induced increase in Glu/Glx within the visual cortex; however, this finding was not linked to any visual stimuli task, but rather to pain, learning, and motor tasks. Additionally, many of the studies included in the review were conducted at 7T, offering

increased sensitivity for detecting changes in Glu/Glx. Nonetheless, several studies have demonstrated changes in Glu/Glx at 3T (e.g., [Gutzeit et al., 2013, Cleve et al., 2017, Apšvalka et al., 2015]). Regarding our GABA+ findings, the same meta-analysis [Pasanta et al., 2023] reported no task-dependent change in GABA within the visual cortex. This may be attributable to technical difficulties associated with capturing GABA levels using MRS at 3T due to its low concentration and signal overlap with more abundant metabolites [Pasanta et al., 2023]. Nevertheless, it is worth noting that several studies have successfully reported changes in GABA at 3T using different paradigms and/or regions of interest (e.g., [Floyer-Lea et al., 2006, Sampaio-Baptista et al., 2015, Stagg et al., 2011]).

Another reason we may not have found changes in Glx or GABA+ may be due to use of a block-design: collecting 24 minutes of rest data, then collecting 24 minutes of movie-watching data. While a block design has the advantage of a more robust metabolite quantification due to greater signal averaging, brain homeostasis during these long blocks may lead to an erasure of any real metabolic changes [Mangia et al., 2012, Apšvalka et al., 2015]. Indeed, Pasanta et al. [2023] found the magnitude of effect sizes were observed to be smaller for block designs than event-related designs.

However, it may be possible that our results do support the idea that H and E:I are not directly linked; at least not in a simple manner. This would perhaps not be surprising given the large disparity of findings in the literature, especially with regard to the directionality and linearity of the proposed E:I-Hurst relationship [Liang et al., 2024, Poil et al., 2012, Lombardi et al., 2017, Baumgarten and Bornholdt, 2019, Bruining et al., 2020, Trakoshis et al., Gao et al., 2017] (see Table 3). The heterogeneity across these E:I-Hurst studies highlights the challenges of studying this phenomenon as well as the complexity of any potential relationship between these two metrics. It may be that, given the mixed-findings of these studies in combination with our data, an E:I-Hurst relationship — should it exist — may depend in part on how the data is collected. This could include variables such as the experimental setup, sampling methods, or data analysis techniques used. Further research is needed to elucidate the true nature of any potential E:I-Hurst relationship and better understand the complexities involved in studying this phenomenon.

Table 3. Summary of methods for existing E:I-Hurst studies

Citation	Study Type	H Data Type	H Calculation Method	E:I Type	E:I-Hurst Relationship
Poil et al. (2012) Poil et al. (2012)	Computational with in-house simulated	Neuronal avalanche size model	Detrended fluctuation analysis (DFA)	Structural: number of E-to-I neurons	Inverse U

Citation	Study Type	H Data Type	H Calculation Method	E:I Type	E:I-Hurst Relationship
Bruining et al. (2020) Bruining et al. [2020]	Computational model with Poil et al. (2012); modified in-house	Neuronal oscillation amplitude	DFA	Structural: number of E-to-I synapses	Inverse U
Gao et al. (2017) Gao et al. [2017]	Computational in vivo in rats and macaques	Local field potential (LFP)	PSD	Estimated from LFP	Positive linear
Lombardi et al. (2017) Lombardi et al. [2017]	Computational with in-house model	Neuronal avalanche size	PSD	Structural: number of E-to-I neurons	Negative linear
Trakoshis et al. (2020) Trakoshis et al. [2020]	Computational with simulated data; in vivo in mice	fMRI BOLD signal	Wavelet-based maximum likelihood method	E-to-I synaptic conductance	Positive linear

Finally, it is also possible that while an E:I-Hurst relationship exists, it is not observed within the visual cortex. This theory seems plausible given that MRS studies of disrupted E:I, mostly conducted within the context of adult autism spectrum disorder, have found changes in E:I within other brain regions such as the anterior cingulate cortex, frontal lobe, or temporal lobe [Ajram et al., 2019]. Moreover, findings with reference to changes in excitatory or inhibitory neurotransmitters within the visual cortex tend to be difficult to capture, perhaps indicating that E:I shows less changes in this region [Pasanta et al., 2023]. However, this would suggest that the E:I-H relationship would be region dependent, and therefore not a generalizable theory as it is often portrayed.

4.1 Limitations and Strengths

Beyond the limitations already mentioned (field strength, visual cortex, passive task, block design), another limitation was our small sample size. As this was a pilot study, 26 participants were initially scanned. Once individuals were excluded for poor MRI quality, only 19 participants' data were analyzed. With this small sample size, it is difficult to make conclusions about a concept as complex as the E:I-Hurst relationship. We hope that by publishing our work, future researchers can use our reported effect sizes to calculate potential sample sizes. We would also like to list some of the strengths of our study, which include: using sLASER (as opposed to PRESS), which

has been shown to have enhanced detection of complex multiplets such as Glu [Wilson et al., 2019]; using the J-editing sequence MEGA-PRESS for improved GABA detection [Peek et al., 2023]; using a large MRS voxel size (~22 ml) as per consensus recommendations [Peek et al., 2020, Choi et al., 2021, Lin et al., 2021]; measuring H within the same region as our single-voxel MRS; and using multi-echo fMRI for improved motion artifact regression [Kundu et al., 2017].

4.2 Lessons for Future Researchers

Finally, we hope that by publishing our findings, we can provide some guidance to future researchers. The following is a non-exhaustive list of suggestions for future work:

- future studies should consider using ultra-high-field 7T MRI, which provides improved spectral resolution and more reliable detection of Glu and GABA compared to conventional 3T MRI;
- examining paradigms that have consistently demonstrated alterations in these metabolites, such as pain studies, may enhance the likelihood of detecting changes in Glu and GABA [Archibald et al., 2020, Cleve et al., 2017, Gutzeit et al., 2013].
- exploring brain regions beyond the visual cortex, such as the anterior cingulate cortex, which is commonly implicated in pain processing [Archibald et al., 2020, Mullins et al., 2005, Gussew et al., 2010, Gutzeit et al., 2011];
- including a more diverse participant sample — beyond healthy controls — may help capture a wider range of H and E:I values, potentially improving sensitivity to metabolite-related changes;
- increasing sample size in order to detect small effect sizes;
- using an event-related design, as opposed to the block design we used, may provide more sensitivity to detecting rapid and transient neural responses due to its ability to isolate specific events within the scan session [Mullins, 2018]. However, see Pasanta et al. [2023] for a longer discussion and possible downsides to this approach;
- and finally, using a combined fMRI-MRS sequence [Ip et al., 2017, Dwyer et al., 2021] to measure BOLD and Glu/GABA near-simultaneously.

Together, these considerations may help in overcoming the limitations observed in the present study and contribute to a clearer understanding of the potential relationship between E:I and H.

5 Conclusion

In conclusion, our findings do not support a relationship between H and E:I in the visual cortex either during rest or during movie-watching at 3T in humans. In addition, while we found a task-related change in H, we did not find any changes in Glu, GABA, or E:I between movie and rest. Comparing our findings to the broader literature, E:I balance may be too subtle to be detected with conventional 3T MRS methods. With regards to the broader E:I-Hurst relationship, we similarly suggest that either this relationship is insufficiently captured with our methods, or that the

relationship between these two variables may be more complex than originally envisaged — perhaps they are not directly related, but rather connected through other mediating variables in a non-linear fashion. To our knowledge, this is the first *in vivo* human study to test for this relationship. It is our hope that as the literature grows, more authors will examine this relationship with respect to other brain regions and using other methods, and will use the lessons learned in this study to inform their own. Hopefully then it will be possible to corroborate findings to probe the complex relationships that may exist with regards to H and E:I in the human brain.

Data availability statement

All code used in this paper is available at github.com/WeberLab/EI_Hurst_Analysis. The data used in this paper is available by contacting the author. The manuscript was written in a ‘reproducible manner’. The entire manuscript, including statistics reported, figures, and tables, can be reproduced here: weberlab.github.io/EI_Hurst_Manuscript/

Competing interests

The authors declare they have no known competing interests.

Author contributions

LS performed data curation, formal analysis, investigation, software, visualization, and wrote the original draft. AMW performed, conceptualization, data curation, formal analysis, funding acquisition, investigation, methodology, project administration, resources, supervision, validation, visualization, and writing - review & editing.

Acknowledgements

The work presented in this paper was supported in part by

References

Laura A. Ajram, Andreia C. Pereira, Alice M. S. Durieux, Hester E. Velthius, Marija M. Petrinovic, and Grainne M. McAlonan. The contribution of [1H] magnetic resonance spectroscopy to the study of excitation-inhibition in autism. *Progress in Neuro-Psychopharmacology and Biological Psychiatry*, 89:236–244, March 2019. ISSN 0278-5846. doi: 10.1016/j.pnpbp.2018.09.010.

Dace Apšvalka, Andrew Gadic, Matthew Clemence, and Paul G. Mullins. Event-related dynamics of glutamate and BOLD effects measured using functional magnetic resonance spectroscopy (fMRS) at 3T in a repetition suppression paradigm. *NeuroImage*, 118:292–300, September 2015. ISSN 1095-9572. doi: 10.1016/j.neuroimage.2015.06.015.

- J. Archibald, E. L. MacMillan, C. Graf, P. Kozlowski, C. Laule, and J. L. K. Kramer. Metabolite activity in the anterior cingulate cortex during a painful stimulus using functional MRS. *Scientific Reports*, 10(1):19218, November 2020. ISSN 2045-2322. doi: 10.1038/s41598-020-76263-3.
- B. B. Avants, C. L. Epstein, M. Grossman, and J. C. Gee. Symmetric diffeomorphic image registration with cross-correlation: Evaluating automated labeling of elderly and neurodegenerative brain. *Medical Image Analysis*, 12(1):26–41, February 2008. ISSN 1361-8423. doi: 10.1016/j.media.2007.06.004.
- Michel Baranger. Chaos, Complexity, and Entropy: A physics talk for non-physicists. *New England Complex Systems Institute*, April 2000.
- Anna Barnes, Edward T. Bullmore, and John Suckling. Endogenous Human Brain Dynamics Recover Slowly Following Cognitive Effort. *PLoS ONE*, 4(8):e6626, August 2009. ISSN 1932-6203. doi: 10.1371/journal.pone.0006626.
- Danielle S. Bassett and Michael S. Gazzaniga. Understanding complexity in the human brain. *Trends in cognitive sciences*, 15(5):200–209, May 2011. ISSN 1364-6613. doi: 10.1016/j.tics.2011.03.006.
- Lorenz Baumgarten and Stefan Bornholdt. Critical excitation-inhibition balance in dense neural networks. *Physical Review E*, 100(1):010301, July 2019. doi: 10.1103/PhysRevE.100.010301.
- Claude Bédard and Alain Destexhe. Macroscopic Models of Local Field Potentials and the Apparent 1/f Noise in Brain Activity. *Biophysical Journal*, 96(7):2589–2603, April 2009. ISSN 00063495. doi: 10.1016/j.bpj.2008.12.3951.
- John Beggs and Nicholas Timme. Being Critical of Criticality in the Brain. *Frontiers in Physiology*, 3, 2012. ISSN 1664-042X.
- Arnaud Boré, Samuel Guay, Christophe Bedetti, Steven Meisler, and Nick GuenTher. Dcm2Bids. Zenodo, October 2023.
- Hilgo Bruining, Richard Hardstone, Erika L. Juarez-Martinez, Jan Sprengers, Arthur-Ervin Avramiea, Sonja Simpraga, Simon J. Houtman, Simon-Shlomo Poil, Eva Dallares, Satu Palva, Bob Oranje, J. Matias Palva, Huibert D. Mansvelder, and Klaus Linkenkaer-Hansen. Measurement of excitation-inhibition ratio in autism spectrum disorder using critical brain dynamics. *Scientific Reports*, 10(1):9195, June 2020. ISSN 2045-2322. doi: 10.1038/s41598-020-65500-4.
- Ed Bullmore, Jalal Fadili, Voichita Maxim, Levent Şendur, Brandon Whitcher, John Suckling, Michael Brammer, and Michael Breakspear. Wavelets and functional magnetic resonance imaging of the human brain. *NeuroImage*, 23:S234–S249, January 2004. ISSN 1053-8119. doi: 10.1016/j.neuroimage.2004.07.012.
- E.T. Bullmore, M.J. Brammer, P. Bourlon, G. Alarcon, C.E. Polkey, R. Elwes, and C.D. Binnie. Fractal analysis of electroencephalographic signals intracerebrally

- recorded during 35 epileptic seizures: Evaluation of a new method for synoptic visualisation of ictal events. *Electroencephalography and Clinical Neurophysiology*, 91(5):337–345, November 1994. ISSN 00134694. doi: 10.1016/0013-4694(94)00181-2.
- Olivia Campbell, Tamara Vanderwal, and Alexander Mark Weber. Fractal-Based Analysis of fMRI BOLD Signal During Naturalistic Viewing Conditions. *Frontiers in Physiology*, 12, 2022. ISSN 1664-042X.
- Olivia Lauren Campbell and Alexander Mark Weber. Monofractal analysis of functional magnetic resonance imaging: An introductory review. *Human Brain Mapping*, 43(8):2693–2706, March 2022. ISSN 1065-9471. doi: 10.1002/hbm.25801.
- F. Caserta, W.D. Eldred, E. Fernandez, R.E. Hausman, L.R. Stanford, S.V. Bulderev, S. Schwarzer, and H.E. Stanley. Determination of fractal dimension of physiologically characterized neurons in two and three dimensions. *Journal of Neuroscience Methods*, 56(2):133–144, February 1995. ISSN 01650270. doi: 10.1016/0165-0270(94)00115-W.
- In-Young Choi, Ovidiu C. Andronesi, Peter Barker, Wolfgang Bogner, Richard A. E. Edden, Lana G. Kaiser, Phil Lee, Małgorzata Marjańska, Melissa Terpstra, and Robin A. de Graaf. Spectral editing in ^1H magnetic resonance spectroscopy: Experts' consensus recommendations. *NMR in Biomedicine*, 34(5):e4411, 2021. ISSN 1099-1492. doi: 10.1002/nbm.4411.
- Nathan W. Churchill, Robyn Spring, Cheryl Grady, Bernadine Cimprich, Mary K. Askren, Patricia A. Reuter-Lorenz, Mi Sook Jung, Scott Peltier, Stephen C. Strother, and Marc G. Berman. The suppression of scale-free fMRI brain dynamics across three different sources of effort: Aging, task novelty and task difficulty. *Scientific Reports*, 6(1):30895, August 2016. ISSN 2045-2322. doi: 10.1038/srep30895.
- Philippe Ciuciu, Patrice Abry, and Biyu J. He. Interplay between functional connectivity and scale-free dynamics in intrinsic fMRI networks. *NeuroImage*, 95:248–263, July 2014. ISSN 1095-9572. doi: 10.1016/j.neuroimage.2014.03.047.
- Marianne Cleve, Alexander Gussew, Gerd Wagner, Karl-Jürgen Bär, and Jürgen R. Reichenbach. Assessment of intra- and inter-regional interrelations between GABA+, Glx and BOLD during pain perception in the human brain - A combined ^1H fMRS and fMRI study. *Neuroscience*, 365:125–136, December 2017. ISSN 1873-7544. doi: 10.1016/j.neuroscience.2017.09.037.
- Huw Cordey. Jungles, April 2019.
- Robert W. Cox. AFNI: Software for Analysis and Visualization of Functional Magnetic Resonance Neuroimages. *Computers and Biomedical Research*, 29(3):162–173, June 1996. ISSN 0010-4809. doi: 10.1006/cbmr.1996.0014.
- A. M. Dale, B. Fischl, and M. I. Sereno. Cortical surface-based analysis. I. Segmentation and surface reconstruction. *NeuroImage*, 9(2):179–194, February 1999. ISSN 1053-8119. doi: 10.1006/nimg.1998.0395.

Gustavo Deco, Viktor K. Jirsa, and Anthony R. McIntosh. Resting brains never rest: Computational insights into potential cognitive architectures. *Trends in Neurosciences*, 36(5):268–274, May 2013. ISSN 0166-2236. doi: 10.1016/j.tins.2013.03.001.

Olga Dona, Geoffrey B. Hall, and Michael D. Noseworthy. Temporal fractal analysis of the rs-BOLD signal identifies brain abnormalities in autism spectrum disorder. *PLOS ONE*, 12(12):e0190081, December 2017a. ISSN 1932-6203. doi: 10.1371/journal.pone.0190081.

Olga Dona, Michael D. Noseworthy, Carol DeMatteo, and John F. Connolly. Fractal Analysis of Brain Blood Oxygenation Level Dependent (BOLD) Signals from Children with Mild Traumatic Brain Injury (mTBI). *PLOS ONE*, 12(1):e0169647, January 2017b. ISSN 1932-6203. doi: 10.1371/journal.pone.0169647.

Jianxin Dong, Bin Jing, Xiangyu Ma, Han Liu, Xiao Mo, and Haiyun Li. Hurst Exponent Analysis of Resting-State fMRI Signal Complexity across the Adult Lifespan. *Frontiers in Neuroscience*, 12, 2018. ISSN 1662-453X.

Eugene P. Duff, Leigh A. Johnston, Jinhu Xiong, Peter T. Fox, Iven Mareels, and Gary F. Egan. The power of spectral density analysis for mapping endogenous BOLD signal fluctuations. *Human Brain Mapping*, 29(7):778–790, May 2008. ISSN 1065-9471. doi: 10.1002/hbm.20601.

Elizabeth DuPre, Taylor Salo, Zaki Ahmed, Peter A. Bandettini, Katherine L. Botterhorn, César Caballero-Gaudes, Logan T. Dowdle, Javier Gonzalez-Castillo, Stephan Heunis, Prantik Kundu, Angela R. Laird, Ross Markello, Christopher J. Markiewicz, Stefano Moia, Isla Staden, Joshua B. Teves, Eneko Uruñuela, Maryam Vaziri-Pashkam, Kirstie Whitaker, and Daniel A. Handwerker. TE-dependent analysis of multi-echo fMRI with *tedana*. *Journal of Open Source Software*, 6(66):3669, October 2021. ISSN 2475-9066. doi: 10.21105/joss.03669.

Gerard Eric Dwyer, Alexander R. Craven, Justyna Bereśniewicz, Katarzyna Kazimierczak, Lars Ersland, Kenneth Hugdahl, and Renate Grüner. Simultaneous Measurement of the BOLD Effect and Metabolic Changes in Response to Visual Stimulation Using the MEGA-PRESS Sequence at 3 T. *Frontiers in Human Neuroscience*, 15:644079, March 2021. ISSN 1662-5161. doi: 10.3389/fnhum.2021.644079.

A. Eke, P. Herman, L. Kocsis, and L. R. Kozak. Fractal characterization of complexity in temporal physiological signals. *Physiological Measurement*, 23(1):R1–38, February 2002. ISSN 0967-3334. doi: 10.1088/0967-3334/23/1/201.

Oscar Esteban, Christopher J. Markiewicz, Ross W. Blair, Craig A. Moodie, A. Ilkay Isik, Asier Erramuzpe, James D. Kent, Mathias Goncalves, Elizabeth DuPre, Madeleine Snyder, Hiroyuki Oya, Satrajit S. Ghosh, Jessey Wright, Joke Durnez, Russell A. Poldrack, and Krzysztof J. Gorgolewski. fMRIPrep: A robust preprocessing pipeline for functional MRI. *Nature Methods*, 16(1):111–116, January 2019. ISSN 1548-7105. doi: 10.1038/s41592-018-0235-4.

M.J. Fadili and E.T. Bullmore. Wavelet-Generalized Least Squares: A New BLU Estimator of Linear Regression Models with 1/f Errors. *NeuroImage*, 15(1):217–232, January 2002. ISSN 10538119. doi: 10.1006/nimg.2001.0955.

Anna Foyer-Lea, Marzena Wylezinska, Tamas Kincses, and Paul M. Matthews. Rapid Modulation of GABA Concentration in Human Sensorimotor Cortex During Motor Learning. *Journal of Neurophysiology*, 95(3):1639–1644, March 2006. ISSN 0022-3077, 1522-1598. doi: 10.1152/jn.00346.2005.

David Freedman, Robert Pisani, and Roger Purves. *Statistics*, volume 4. W. W. Norton & Company, New York, 2007. ISBN 0-393-93043-2.

Karl Friston, John Ashburner, Stefan Kiebel, Thomas Nichols, and Williams Penny. *Statistical Parametric Mapping: The Analysis of Functional Brain Images*. Elsevier Ltd., 2007. ISBN 978-0-12-372560-8.

Richard Gao, Erik J. Peterson, and Bradley Voytek. Inferring synaptic excitation/inhibition balance from field potentials. *NeuroImage*, 158:70–78, September 2017. ISSN 1053-8119. doi: 10.1016/j.neuroimage.2017.06.078.

Charles Gasparovic, Tao Song, Deidre Devier, H. Jeremy Bockholt, Arvind Caprihan, Paul G. Mullins, Stefan Posse, Rex E. Jung, and Leslie A. Morrison. Use of tissue water as a concentration reference for proton spectroscopic imaging. *Magnetic Resonance in Medicine*, 55(6):1219–1226, 2006. ISSN 1522-2594. doi: 10.1002/mrm.20901.

Krzysztof J. Gorgolewski, Tibor Auer, Vince D. Calhoun, R. Cameron Craddock, Samir Das, Eugene P. Duff, Guillaume Flandin, Satrajit S. Ghosh, Tristan Glatard, Yaroslav O. Halchenko, Daniel A. Handwerker, Michael Hanke, David Keator, Xiangrui Li, Zachary Michael, Camille Maumet, B. Nolan Nichols, Thomas E. Nichols, John Pellman, Jean-Baptiste Poline, Ariel Rokem, Gunnar Schaefer, Vanessa Sochat, William Triplett, Jessica A. Turner, Gaël Varoquaux, and Russell A. Poldrack. The brain imaging data structure, a format for organizing and describing outputs of neuroimaging experiments. *Scientific Data*, 3(1):160044, June 2016a. ISSN 2052-4463. doi: 10.1038/sdata.2016.44.

Krzysztof J. Gorgolewski, Oscar Esteban, Christopher Burns, Erik Ziegler, Basile Pinsard, Cindee Madison, Michael Waskom, David Gage Ellis, Dav Clark, Michael Dayan, Alexandre Manhães-Savio, Michael Philipp Notter, Hans Johnson, Blake E Dewey, Yaroslav O. Halchenko, Carlo Hamalainen, Anisha Keshavan, Daniel Clark, Julia M. Huntenburg, Michael Hanke, B. Nolan Nichols, Demian Wassermann, Arman Eshaghi, Christopher Markiewicz, Gael Varoquaux, Benjamin Acland, Jessica Forbes, Ariel Rokem, Xiang-Zhen Kong, Alexandre Gramfort, Jens Kleesiek, Alexander Schaefer, Sharad Sikka, Martin Felipe Perez-Guevara, Tristan Glatard, Shariq Iqbal, Siqi Liu, David Welch, Paul Sharp, Joshua Warner, Erik Kastman, Leonie Lampe, L. Nathan Perkins, R. Cameron Craddock, René Küttner, Dmytro Bielievtsov, Daniel Geisler, Stephan Gerhard, Franziskus Liem, Janosch Linkersdörfer, Daniel S. Margulies, Sami Kristian Andberg, Jörg Stadler, Christopher John Steele, William Broderick, Gavin Cooper, Andrew Floren, Lijie Huang,

Ivan Gonzalez, Daniel McNamee, Dimitri Papadopoulos Orfanos, John Pellman, William Triplett, and Satrajit Ghosh. Nipype: A flexible, lightweight and extensible neuroimaging data processing framework in Python. 0.12.0-rc1. Zenodo, April 2016b.

Alexander Gussew, Reinhart Rzanny, Marko Erdtel, Hans C. Scholle, Werner A. Kaiser, Hans J. Mentzel, and Jürgen R. Reichenbach. Time-resolved functional ^1H MR spectroscopic detection of glutamate concentration changes in the brain during acute heat pain stimulation. *NeuroImage*, 49(2):1895–1902, January 2010. ISSN 1095-9572. doi: 10.1016/j.neuroimage.2009.09.007.

A. Gutzeit, D. Meier, M. L. Meier, C. von Weymarn, D. A. Ettlin, N. Graf, J. M. Froehlich, C. A. Binkert, and M. Brügger. Insula-specific responses induced by dental pain. A proton magnetic resonance spectroscopy study. *European Radiology*, 21(4):807–815, April 2011. ISSN 1432-1084. doi: 10.1007/s00330-010-1971-8.

Andreas Gutzeit, Dieter Meier, Johannes M. Froehlich, Klaus Hergan, Sebastian Kos, Constantin V Weymarn, Kai Lutz, Dominik Ettlin, Christoph A. Binkert, Jochen Mutschler, Sabine Sartoretti-Schefer, and Mike Brügger. Differential NMR spectroscopy reactions of anterior/posterior and right/left insular subdivisions due to acute dental pain. *European Radiology*, 23(2):450–460, February 2013. ISSN 1432-1084. doi: 10.1007/s00330-012-2621-0.

Ashley D. Harris, Nicolaas A.J. Puts, Peter B. Barker, and Richard A.E. Edden. Spectral-Editing Measurements of GABA in the Human Brain with and without Macromolecule Suppression. *Magnetic resonance in medicine*, 74(6):1523–1529, December 2015. ISSN 0740-3194. doi: 10.1002/mrm.25549.

Ashley D. Harris, Muhammad G. Saleh, and Richard A. E. Edden. Edited ^1H magnetic resonance spectroscopy *in vivo*: Methods and metabolites. *Magnetic Resonance in Medicine*, 77(4):1377–1389, April 2017. ISSN 1522-2594. doi: 10.1002/mrm.26619.

Uri Hasson, Rafael Malach, and David J. Heeger. Reliability of cortical activity during natural stimulation. *Trends in Cognitive Sciences*, 14(1):40–48, January 2010. ISSN 1364-6613. doi: 10.1016/j.tics.2009.10.011.

Biyu J. He. Scale-Free Properties of the Functional Magnetic Resonance Imaging Signal during Rest and Task. *Journal of Neuroscience*, 31(39):13786–13795, September 2011. ISSN 0270-6474, 1529-2401. doi: 10.1523/JNEUROSCI.2111-11.2011.

Steve C. N. Hui, Muhammad G. Saleh, Helge J. Zöllner, Georg Oeltzscher, Hongli Fan, Yue Li, Yulu Song, Hangyi Jiang, Jamie Near, Hanzhang Lu, Susumu Mori, and Richard A. E. Edden. MRSCloud: A cloud-based MRS tool for basis set simulation. *Magnetic Resonance in Medicine*, 88(5):1994–2004, 2022. ISSN 1522-2594. doi: 10.1002/mrm.29370.

I. Betina Ip, Adam Berrington, Aaron T. Hess, Andrew J. Parker, Uzay E. Emir, and Holly Bridge. Combined fMRI-MRS acquires simultaneous glutamate and BOLD-fMRI signals in the human brain. *NeuroImage*, 155:113–119, July 2017. ISSN 1095-9572. doi: 10.1016/j.neuroimage.2017.04.030.

Mark Jenkinson, Peter Bannister, Michael Brady, and Stephen Smith. Improved optimization for the robust and accurate linear registration and motion correction of brain images. *NeuroImage*, 17(2):825–841, October 2002. ISSN 1053-8119. doi: 10.1016/s1053-8119(02)91132-8.

Bin Jing, Zhuqing Long, Han Liu, Huagang Yan, Jianxin Dong, Xiao Mo, Dan Li, Chunhong Liu, and Haiyun Li. Identifying current and remitted major depressive disorder with the Hurst exponent: A comparative study on two automated anatomical labeling atlases. *Oncotarget*, 8(52):90452–90464, August 2017. ISSN 1949-2553. doi: 10.18632/oncotarget.19860.

Eunchai Kang, Juan Song, Yuting Lin, Jaesuk Park, Jennifer H. Lee, Qassim Hussani, Yan Gu, Shaoyu Ge, Weidong Li, Kuei-sen Hsu, Benedikt Berninger, Kimberly M. Christian, Hongjun Song, and Guo-li Ming. Interplay between a Mental Disorder Risk Gene and Developmental Polarity Switch of GABA Action Leads to Excitation-Inhibition Imbalance. *Cell Reports*, 28(6):1419–1428.e3, August 2019. ISSN 22111247. doi: 10.1016/j.celrep.2019.07.024.

Arno Klein, Satrajit S. Ghosh, Forrest S. Bao, Joachim Giard, Yrjö Häme, Eliezer Stavsky, Noah Lee, Brian Rossa, Martin Reuter, Elias Chaibub Neto, and Anisha Keshavan. Mindboggling morphometry of human brains. *PLoS computational biology*, 13(2):e1005350, February 2017. ISSN 1553-7358. doi: 10.1371/journal.pcbi.1005350.

Prantik Kundu, Valerie Voon, Priti Balchandani, Michael V. Lombardo, Benedikt A. Poser, and Peter A. Bandettini. Multi-echo fMRI: A review of applications in fMRI denoising and analysis of BOLD signals. *NeuroImage*, 154:59–80, July 2017. ISSN 1053-8119. doi: 10.1016/j.neuroimage.2017.03.033.

Meng-Chuan Lai, Michael V. Lombardo, Bhismadev Chakrabarti, Susan A. Sadek, Greg Pasco, Sally J. Wheelwright, Edward T. Bullmore, Simon Baron-Cohen, and John Suckling. A Shift to Randomness of Brain Oscillations in People with Autism. *Biological Psychiatry*, 68(12):1092–1099, December 2010. ISSN 0006-3223. doi: 10.1016/j.biopsych.2010.06.027.

Julie C. Lauterborn, Pietro Scaduto, Conor D. Cox, Anton Schulmann, Gary Lynch, Christine M. Gall, C. Dirk Keene, and Agenor Limon. Increased excitatory to inhibitory synaptic ratio in parietal cortex samples from individuals with Alzheimer’s disease. *Nature Communications*, 12(1):2603, May 2021. ISSN 2041-1723. doi: 10.1038/s41467-021-22742-8.

Xiangrui Li, Paul S. Morgan, John Ashburner, Jolinda Smith, and Christopher Rorden. The first step for neuroimaging data analysis: DICOM to NIfTI conversion. *Journal*

of Neuroscience Methods, 264:47–56, May 2016. ISSN 1872-678X. doi: 10.1016/j.jneumeth.2016.03.001.

Junhao Liang, Zhuda Yang, and Changsong Zhou. Excitation–Inhibition Balance, Neural Criticality, and Activities in Neuronal Circuits. *The Neuroscientist*, page 10738584231221766, January 2024. ISSN 1073-8584. doi: 10.1177/10738584231221766.

Alexander Lin, Ovidiu Andronesi, Wolfgang Bogner, In-Young Choi, Eduardo Coello, Cristina Cudalbu, Christoph Juchem, Graham J. Kemp, Roland Kreis, Martin Kršák, Phil Lee, Andrew A. Maudsley, Martin Meyerspeer, Vladamir Mlynarik, Jamie Near, Gülin Öz, Aimie L. Peek, Nicolaas A. Puts, Eva-Maria Ratai, Ivan Tkáč, Paul G. Mullins, and Experts’ Working Group on Reporting Standards for MR Spectroscopy. Minimum Reporting Standards for in vivo Magnetic Resonance Spectroscopy (MRSinMRS): Experts’ consensus recommendations. *NMR in biomedicine*, 34(5):e4484, May 2021. ISSN 1099-1492. doi: 10.1002/nbm.4484.

F. Lombardi, H. J. Herrmann, and L. de Arcangelis. Balance of excitation and inhibition determines 1/f power spectrum in neuronal networks. *Chaos: An Interdisciplinary Journal of Nonlinear Science*, 27(4):047402, March 2017. ISSN 1054-1500. doi: 10.1063/1.4979043.

Steven B. Lowen, Sydney S. Cash, Mu-ming Poo, and Malvin C. Teich. Quantal Neurotransmitter Secretion Rate Exhibits Fractal Behavior. *The Journal of Neuroscience*, 17(15):5666–5677, August 1997. ISSN 0270-6474, 1529-2401. doi: 10.1523/JNEUROSCI.17-15-05666.1997.

Silvia Mangia, Federico Giove, and Mauro Dinuzzo. Metabolic pathways and activity-dependent modulation of glutamate concentration in the human brain. *Neurochemical Research*, 37(11):2554–2561, November 2012. ISSN 1573-6903. doi: 10.1007/s11064-012-0848-4.

Voichița Maxim, Levent Şendur, Jalal Fadili, John Suckling, Rebecca Gould, Rob Howard, and Ed Bullmore. Fractional Gaussian noise, functional MRI and Alzheimer’s disease. *NeuroImage*, 25(1):141–158, March 2005. ISSN 1053-8119. doi: 10.1016/j.neuroimage.2004.10.044.

Alberto Mazzoni, Frédéric D. Broccard, Elizabeth Garcia-Perez, Paolo Bonifazi, Maria Elisabetta Ruaro, and Vincent Torre. On the Dynamics of the Spontaneous Activity in Neuronal Networks. *PLoS ONE*, 2(5):e439, May 2007. ISSN 1932-6203. doi: 10.1371/journal.pone.0000439.

M. Mescher, H. Merkle, J. Kirsch, M. Garwood, and R. Gruetter. Simultaneous in vivo spectral editing and water suppression. *NMR in biomedicine*, 11(6):266–272, October 1998. ISSN 0952-3480. doi: 10.1002/(sici)1099-1492(199810)11:6<266::aid-nbm530>3.0.co;2-j.

Mark Mikkelsen, Peter B. Barker, Pallab K. Bhattacharyya, Maiken K. Brix, Pieter F. Buur, Kim M. Cecil, Kimberly L. Chan, David Y. T. Chen, Alexander R. Craven,

Koen Cuypers, Michael Dacko, Niall W. Duncan, Ulrike Dydak, David A. Edmondson, Gabriele Ende, Lars Ersland, Fei Gao, Ian Greenhouse, Ashley D. Harris, Naying He, Stefanie Heba, Nigel Hoggard, Tun-Wei Hsu, Jacobus F. A. Jansen, Alayar Kangarlu, Thomas Lange, R. Marc Lebel, Yan Li, Chien-Yuan E. Lin, Jy-Kang Liou, Jiing-Feng Lirng, Feng Liu, Ruoyun Ma, Celine Maes, Marta Moreno-Ortega, Scott O. Murray, Sean Noah, Ralph Noeske, Michael D. Noseworthy, Georg Oeltzschnner, James J. Prisciandaro, Nicolaas A. J. Puts, Timothy P. L. Roberts, Markus Sack, Napapon Sailasuta, Muhammad G. Saleh, Michael-Paul Schallmo, Nicholas Simard, Stephan P. Swinnen, Martin Tegenthoff, Peter Truong, Guangbin Wang, Iain D. Wilkinson, Hans-Jörg Wittsack, Hongmin Xu, Fuhua Yan, Chencheng Zhang, Vadim Zipunnikov, Helge J. Zöllner, and Richard A. Edden. Big GABA: Edited MR spectroscopy at 24 research sites. *NeuroImage*, 159:32–45, October 2017. ISSN 1053-8119. doi: 10.1016/j.neuroimage.2017.07.021.

Mark Mikkelsen, Daniel L. Rimbault, Peter B. Barker, Pallab K. Bhattacharyya, Maiken K. Brix, Pieter F. Buur, Kim M. Cecil, Kimberly L. Chan, David Y.-T. Chen, Alexander R. Craven, Koen Cuypers, Michael Dacko, Niall W. Duncan, Ulrike Dydak, David A. Edmondson, Gabriele Ende, Lars Ersland, Megan A. Forbes, Fei Gao, Ian Greenhouse, Ashley D. Harris, Naying He, Stefanie Heba, Nigel Hoggard, Tun-Wei Hsu, Jacobus F.A. Jansen, Alayar Kangarlu, Thomas Lange, R. Marc Lebel, Yan Li, Chien-Yuan E. Lin, Jy-Kang Liou, Jiing-Feng Lirng, Feng Liu, Joanna R. Long, Ruoyun Ma, Celine Maes, Marta Moreno-Ortega, Scott O. Murray, Sean Noah, Ralph Noeske, Michael D. Noseworthy, Georg Oeltzschnner, Eric C. Porges, James J. Prisciandaro, Nicolaas A.J. Puts, Timothy P.L. Roberts, Markus Sack, Napapon Sailasuta, Muhammad G. Saleh, Michael-Paul Schallmo, Nicholas Simard, Diederick Stoffers, Stephan P. Swinnen, Martin Tegenthoff, Peter Truong, Guangbin Wang, Iain D. Wilkinson, Hans-Jörg Wittsack, Adam J. Woods, Hongmin Xu, Fuhua Yan, Chencheng Zhang, Vadim Zipunnikov, Helge J. Zöllner, and Richard A.E. Edden. Big GABA II: Water-referenced edited MR spectroscopy at 25 research sites. *NeuroImage*, 191:537–548, May 2019. ISSN 10538119. doi: 10.1016/j.neuroimage.2019.02.059.

Susumu Mori, Dan Wu, Can Ceritoglu, Yue Li, Anthony Kolasny, Marc A. Vaillant, Andreia V. Faria, Kenichi Oishi, and Michael I. Miller. MRICloud: Delivering High-Throughput MRI Neuroinformatics as Cloud-Based Software as a Service. *Computing in Science & Engineering*, 18(5):21–35, September 2016. ISSN 1521-9615. doi: 10.1109/MCSE.2016.93.

Paul G. Mullins. Towards a theory of functional magnetic resonance spectroscopy (fMRS): A meta-analysis and discussion of using MRS to measure changes in neurotransmitters in real time. *Scandinavian Journal of Psychology*, 59(1):91–103, February 2018. ISSN 1467-9450. doi: 10.1111/sjop.12411.

Paul G. Mullins, Laura M. Rowland, Rex E. Jung, and Wilmer L. Sibbitt. A novel technique to study the brain's response to pain: Proton magnetic resonance spectroscopy. *NeuroImage*, 26(2):642–646, June 2005. ISSN 1053-8119. doi: 10.1016/j.neuroimage.2005.02.001.

Miguel A. Muñoz. *Colloquium : Criticality and dynamical scaling in living systems. Reviews of Modern Physics*, 90(3):031001, July 2018. ISSN 0034-6861, 1539-0756. doi: 10.1103/RevModPhys.90.031001.

Georg Oeltzschnner, Helge J. Zöllner, Steve C. N. Hui, Mark Mikkelsen, Muhammad G. Saleh, Sofie Tapper, and Richard A. E. Edden. Osprey: Open-Source Processing, Reconstruction & Estimation of Magnetic Resonance Spectroscopy Data. *Journal of neuroscience methods*, 343:108827, September 2020. ISSN 0165-0270. doi: 10.1016/j.jneumeth.2020.108827.

Gülin Oz and Ivan Tkáč. Short-echo, single-shot, full-intensity proton magnetic resonance spectroscopy for neurochemical profiling at 4 T: Validation in the cerebellum and brainstem. *Magnetic Resonance in Medicine*, 65(4):901–910, April 2011. ISSN 1522-2594. doi: 10.1002/mrm.22708.

Chloe E. Page and Laurence Coutellier. Prefrontal excitatory/inhibitory balance in stress and emotional disorders: Evidence for over-inhibition. *Neuroscience & Biobehavioral Reviews*, 105:39–51, October 2019. ISSN 01497634. doi: 10.1016/j.neubiorev.2019.07.024.

Duanghathai Pasanta, Jason L. He, Talitha Ford, Georg Oeltzschnner, David J. Lythgoe, and Nicolaas A. Puts. Functional MRS studies of GABA and glutamate/Glx – A systematic review and meta-analysis. *Neuroscience & Biobehavioral Reviews*, 144:104940, January 2023. ISSN 01497634. doi: 10.1016/j.neubiorev.2022.104940.

Aimie Laura Peek, Trudy Rebbeck, Nicolaas Aj Puts, Julia Watson, Maria-Eliza R. Aguilera, and Andrew M. Leaver. Brain GABA and glutamate levels across pain conditions: A systematic literature review and meta-analysis of 1H-MRS studies using the MRS-Q quality assessment tool. *NeuroImage*, 210:116532, April 2020. ISSN 1095-9572. doi: 10.1016/j.neuroimage.2020.116532.

A.L. Peek, T.J. Rebbeck, A.M. Leaver, S.L. Foster, K.M. Refshauge, N.A. Puts, and G. Oeltzschnner. A comprehensive guide to MEGA-PRESS for GABA measurement. *Analytical Biochemistry*, 669:115113, May 2023. ISSN 0003-2697. doi: 10.1016/j.ab.2023.115113.

Simon-Shlomo Poil, Richard Hardstone, Huibert D. Mansvelder, and Klaus Linkenkaer-Hansen. Critical-State Dynamics of Avalanches and Oscillations Jointly Emerge from Balanced Excitation/Inhibition in Neuronal Networks. *Journal of Neuroscience*, 32(29):9817–9823, July 2012. ISSN 0270-6474, 1529-2401. doi: 10.1523/JNEUROSCI.5990-11.2012.

S. Posse, S. Wiese, D. Gembris, K. Mathiak, C. Kessler, M. L. Grosse-Ruyken, B. Elghahwagi, T. Richards, S. R. Dager, and V. G. Kiselev. Enhancement of BOLD-contrast sensitivity by single-shot multi-echo functional MR imaging. *Magnetic Resonance in Medicine*, 42(1):87–97, July 1999. ISSN 0740-3194. doi: 10.1002/(sici)1522-2594(199907)42:1<87::aid-mrm13>3.0.co;2-0.

Saadallah Ramadan, Alexander Lin, and Peter Stanwell. Glutamate and Glutamine: A Review of In Vivo MRS in the Human Brain. *NMR in biomedicine*, 26(12): 10.1002/nbm.3045, December 2013. ISSN 0952-3480. doi: 10.1002/nbm.3045.

Reuben Rideaux. No balance between glutamate+glutamine and GABA+ in visual or motor cortices of the human brain: A magnetic resonance spectroscopy study. *NeuroImage*, 237:118191, August 2021. ISSN 1053-8119. doi: 10.1016/j.neuroimage.2021.118191.

Mikail Rubinov, Olaf Sporns, Jean-Philippe Thivierge, and Michael Breakspear. Neurobiologically Realistic Determinants of Self-Organized Criticality in Networks of Spiking Neurons. *PLOS Computational Biology*, 7(6):e1002038, June 2011. ISSN 1553-7358. doi: 10.1371/journal.pcbi.1002038.

Cassandra Sampaio-Baptista, Nicola Filippini, Charlotte J. Stagg, Jamie Near, Jan Scholz, and Heidi Johansen-Berg. Changes in functional connectivity and GABA levels with long-term motor learning. *NeuroImage*, 106:15–20, February 2015. ISSN 10538119. doi: 10.1016/j.neuroimage.2014.11.032.

Alexander Schaefer, Jennifer S. Brach, Subashan Perera, and Ervin Sejdić. A comparative analysis of spectral exponent estimation techniques for $1/f\beta$ processes with applications to the analysis of stride interval time series. *Journal of neuroscience methods*, 222:118–130, January 2014. ISSN 0165-0270. doi: 10.1016/j.jneumeth.2013.10.017.

Stephen M. Smith, Mark Jenkinson, Mark W. Woolrich, Christian F. Beckmann, Timothy E. J. Behrens, Heidi Johansen-Berg, Peter R. Bannister, Marilena De Luca, Ivana Dronjak, David E. Flitney, Rami K. Niazy, James Saunders, John Vickers, Yongyue Zhang, Nicola De Stefano, J. Michael Brady, and Paul M. Matthews. Advances in functional and structural MR image analysis and implementation as FSL. *NeuroImage*, 23 Suppl 1:S208–219, 2004. ISSN 1053-8119. doi: 10.1016/j.neuroimage.2004.07.051.

Vikaas S. Sohal and John L. R. Rubenstein. Excitation-inhibition balance as a framework for investigating mechanisms in neuropsychiatric disorders. *Molecular Psychiatry*, 24(9):1248–1257, September 2019. ISSN 1359-4184, 1476-5578. doi: 10.1038/s41380-019-0426-0.

Moses O. Sokunbi, Victoria B. Gradin, Gordon D. Waiter, George G. Cameron, Trevor S. Ahearn, Alison D. Murray, Douglas J. Steele, and Roger T. Staff. Non-linear Complexity Analysis of Brain fMRI Signals in Schizophrenia. *PLoS ONE*, 9 (5):e95146, May 2014. ISSN 1932-6203. doi: 10.1371/journal.pone.0095146.

Charlotte J. Stagg, Velicia Bachtiar, and Heidi Johansen-Berg. The Role of GABA in Human Motor Learning. *Current Biology*, 21(6):480–484, March 2011. ISSN 09609822. doi: 10.1016/j.cub.2011.01.069.

Jeffrey A. Stanley and Naftali Raz. Functional Magnetic Resonance Spectroscopy: The “New” MRS for Cognitive Neuroscience and Psychiatry Research. *Frontiers in Psychiatry*, 9:76, March 2018. ISSN 1664-0640. doi: 10.3389/fpsyg.2018.00076.

Student. The Probable Error of a Mean. *Biometrika*, 6(1):1–25, 1908. ISSN 0006-3444. doi: 10.2307/2331554.

R Core Team. R: A language and environment for statistical computing. R Foundation for Statistical Computing, 2021.

B. T. Thomas Yeo, Fenna M. Krienen, Jorge Sepulcre, Mert R. Sabuncu, Danial Lashkari, Marisa Hollinshead, Joshua L. Roffman, Jordan W. Smoller, Lilla Zöllei, Jonathan R. Polimeni, Bruce Fischl, Hesheng Liu, and Randy L. Buckner. The organization of the human cerebral cortex estimated by intrinsic functional connectivity. *Journal of Neurophysiology*, 106(3):1125–1165, September 2011. ISSN 0022-3077, 1522-1598. doi: 10.1152/jn.00338.2011.

Yang Tian, Zeren Tan, Hedong Hou, Guoqi Li, Aohua Cheng, Yike Qiu, Kangyu Weng, Chun Chen, and Pei Sun. Theoretical foundations of studying criticality in the brain. *Network Neuroscience*, 6(4):1148–1185, October 2022. ISSN 2472-1751. doi: 10.1162/netn_a_00269.

Stavros Trakoshis, Pablo Martínez-Cañada, Federico Rocchi, Carola Canella, Wonsang You, Bhismadev Chakrabarti, Amber NV Ruigrok, Edward T Bullmore, John Suckling, Marija Markicevic, Valerio Zerbi, Simon Baron-Cohen, Alessandro Gozzi, Meng-Chuan Lai, Stefano Panzeri, and Michael V Lombardo. Intrinsic excitation-inhibition imbalance affects medial prefrontal cortex differently in autistic men versus women. *eLife*, 9:e55684. ISSN 2050-084X. doi: 10.7554/eLife.55684.

Nicholas J Tustison, Brian B Avants, Philip A Cook, Yuanjie Zheng, Alexander Egan, Paul A Yushkevich, and James C Gee. N4ITK: Improved N3 Bias Correction. *IEEE Transactions on Medical Imaging*, 29(6):1310–1320, June 2010. ISSN 0278-0062, 1558-254X. doi: 10.1109/TMI.2010.2046908.

Genoveva Uzunova, Stefano Pallanti, and Eric Hollander. Excitatory/inhibitory imbalance in autism spectrum disorders: Implications for interventions and therapeutics. *The World Journal of Biological Psychiatry*, 17(3):174–186, April 2016. ISSN 1562-2975, 1814-1412. doi: 10.3109/15622975.2015.1085597.

D.C. Van Essen, K. Ugurbil, E. Auerbach, D. Barch, T.E.J. Behrens, R. Bucholz, A. Chang, L. Chen, M. Corbetta, S.W. Curtiss, S. Della Penna, D. Feinberg, M.F. Glasser, N. Harel, A.C. Heath, L. Larson-Prior, D. Marcus, G. Michalareas, S. Moeller, R. Oostenveld, S.E. Petersen, F. Prior, B.L. Schlaggar, S.M. Smith, A.Z. Snyder, J. Xu, and E. Yacoub. The Human Connectome Project: A data acquisition perspective. *NeuroImage*, 62(4):2222–2231, October 2012. ISSN 10538119. doi: 10.1016/j.neuroimage.2012.02.018.

Eva Vico Varela, Guillaume Etter, and Sylvain Williams. Excitatory-inhibitory imbalance in Alzheimer’s disease and therapeutic significance. *Neurobiology of Disease*, 127:605–615, July 2019. ISSN 09699961. doi: 10.1016/j.nbd.2019.04.010.

Pauli Virtanen, Ralf Gommers, Travis E. Oliphant, Matt Haberland, Tyler Reddy, David Cournapeau, Evgeni Burovski, Pearu Peterson, Warren Weckesser, Jonathan Bright, Stéfan J. van der Walt, Matthew Brett, Joshua Wilson, K. Jarrod Millman,

Nikolay Mayorov, Andrew R. J. Nelson, Eric Jones, Robert Kern, Eric Larson, C. J. Carey, İlhan Polat, Yu Feng, Eric W. Moore, Jake VanderPlas, Denis Laxalde, Josef Perktold, Robert Cimrman, Ian Henriksen, E. A. Quintero, Charles R. Harris, Anne M. Archibald, Antônio H. Ribeiro, Fabian Pedregosa, and Paul van Mulbregt. SciPy 1.0: Fundamental algorithms for scientific computing in Python. *Nature Methods*, 17(3):261–272, March 2020. ISSN 1548-7105. doi: 10.1038/s41592-019-0686-2.

Mohammed A. Warsi, William Molloy, and Michael D. Noseworthy. Correlating brain blood oxygenation level dependent (BOLD) fractal dimension mapping with magnetic resonance spectroscopy (MRS) in Alzheimer’s disease. *Magnetic Resonance Materials in Physics, Biology and Medicine*, 25(5):335–344, October 2012. ISSN 0968-5243, 1352-8661. doi: 10.1007/s10334-012-0312-0.

Maobin Wei, Jiaolong Qin, Rui Yan, Haoran Li, Zhijian Yao, and Qing Lu. Identifying major depressive disorder using Hurst exponent of resting-state brain networks. *Psychiatry Research: Neuroimaging*, 214(3):306–312, December 2013. ISSN 0925-4927. doi: 10.1016/j.pscychresns.2013.09.008.

P. Welch. The use of fast Fourier transform for the estimation of power spectra: A method based on time averaging over short, modified periodograms. *IEEE Transactions on Audio and Electroacoustics*, 15(2):70–73, June 1967. ISSN 0018-9278. doi: 10.1109/TAU.1967.1161901.

Martin Wilson, Ovidiu Andronesi, Peter B. Barker, Robert Bartha, Alberto Bizzi, Patrick J. Bolan, Kevin M. Brindle, In-Young Choi, Cristina Cudalbu, Ulrike Dydak, Uzay E. Emir, Ramon G. Gonzalez, Stephan Gruber, Rolf Gruetter, Rakesh K. Gupta, Arend Heerschap, Anke Henning, Hoby P. Hetherington, Petra S. Huppi, Ralph E. Hurd, Kejal Kantarci, Risto A Kauppinen, Dennis W. J. Klomp, Roland Kreis, Marijn J. Kruiskamp, Martin O. Leach, Alexander P. Lin, Peter R. Luijten, Małgorzata Marjańska, Andrew A. Maudsley, Dieter J. Meyerhoff, Carolyn E. Mountford, Paul G. Mullins, James B. Murdoch, Sarah J. Nelson, Ralph Noeske, Gülin Öz, Julie W. Pan, Andrew C. Peet, Harish Poptani, Stefan Posse, Eva-Maria Ratai, Nouha Salibi, Tom W. J. Scheenen, Ian C. P. Smith, Brian J. Soher, Ivan Tkáč, Daniel B. Vigneron, and Franklyn A. Howe. Methodological consensus on clinical proton MRS of the brain: Review and recommendations. *Magnetic Resonance in Medicine*, 82(2):527–550, August 2019. ISSN 0740-3194, 1522-2594. doi: 10.1002/mrm.27742.

Alle Meije Wink, Frédéric Bernard, Raymond Salvador, Ed Bullmore, and John Suckling. Age and cholinergic effects on hemodynamics and functional coherence of human hippocampus. *Neurobiology of Aging*, 27(10):1395–1404, October 2006. ISSN 0197-4580. doi: 10.1016/j.neurobiolaging.2005.08.011.

Alle-Meije Wink, Ed Bullmore, Anna Barnes, Frederic Bernard, and John Suckling. Monofractal and multifractal dynamics of low frequency endogenous brain oscillations in functional MRI. *Human Brain Mapping*, 29(7):791–801, July 2008. ISSN 1065-9471, 1097-0193. doi: 10.1002/hbm.20593.

E. Zarahn, G.K. Aguirre, and M. D'Esposito. Empirical Analyses of BOLD fMRI Statistics. *NeuroImage*, 5(3):179–197, April 1997. ISSN 10538119. doi: 10.1006/nimg.1997.0263.

Y. Zhang, M. Brady, and S. Smith. Segmentation of brain MR images through a hidden Markov random field model and the expectation-maximization algorithm. *IEEE Transactions on Medical Imaging*, 20(1):45–57, January 2001. ISSN 02780062. doi: 10.1109/42.906424.

Vincent Zimmern. Why Brain Criticality Is Clinically Relevant: A Scoping Review. *Frontiers in Neural Circuits*, 14, 2020. ISSN 1662-5110.